

M. A. Deyab*, A. S. Fouda and S. Abdel-Fattah

New Heterocyclic Derivative to Stop Carbon Steel Corrosion

<https://doi.org/10.1515/zpch-2019-1399>

Received February 18, 2019; accepted April 5, 2019

Abstract: The new compound 4-(2-(1,5-dimethyl-3-oxo-2-phenyl-2,3-dihydro-1H-pyrazol-4-yl)hydrazono)-3-methyl-5-oxo-4,5-dihydro-1H-pyrazole-1-carbothioamide (PY) was synthesized. Its anti-corrosion properties for C-steel in acid solution (1.0 M HCl) were evaluated utilize electrochemical tools. The synthesized compound was described using FT-IR and $^1\text{H-NMR}$ analyses. The purity of PY was affirmed by thin-layer chromatography (TLC). The outcome data proved that PY possess adequate anti-corrosion features for C-steel in corrosive solution. The polarization parameters mentioned that the PY is a mixed inhibitor. Inhibition performance obtained by polarization measurements (i.e. 91.5%) are consistent with the one obtained by EIS (i.e. 88.6%). Quantum chemical parameters for PY were studied to supply assist knowledge into the anti-corrosion properties of the new compound.

Keywords: acid solution; corrosion inhibitor; electrochemical; FT-IR; heterocycle.

1 Introduction

Carbon steel, the foremost broadly utilized designing metal, accounts for around 85% of the yearly steel generation around the world. The chemicals compounds play a critical role to conserve the steel from the corrosion in acidic solutions. Generally, the acid inhibitors are organic and inorganic molecules contain nitrogen, sulfur, and/or oxygen atoms [1–3]. The performance of corrosion inhibitors depend on molecular construction of the inhibitors [4–9].

The nitrogen-heterocyclic inhibitors form complex or chelate compounds with iron metal. In addition, the nitrogen atoms in heterocyclic compounds can be

*Corresponding author: M. A. Deyab, Egyptian Petroleum Research Institute (EPRI), PO Box 11727, Nasr City, Cairo, Egypt, Tel.: +201006137150; Fax: +202 22747433, e-mail: hamadadeiab@yahoo.com

A. S. Fouda: Department of Chemistry, Faculty of Science, El-Mansoura University, El-Mansoura, Egypt

S. Abdel-Fattah: Egyptian Petroleum Research Institute (EPRI), PO Box 11727, Nasr City, Cairo, Egypt

simply protonated in acidic solutions to offer strong inhibitory behavior. The heterocyclic inhibitors work by the adsorption and maintain the metal from corrosion by film coverage. The hetero-atoms, such as phosphor, sulfur, nitrogen, oxygen or those containing multiple bonds are considered as adsorption centers [10–12].

Overview of previous works showed that pyrazole derivatives are potent corrosion inhibitors [13–16]. This reinforces our next work to synthesize other new compounds with high efficiency and low toxicity. There is no literature to date about the corrosion inhibitive effect of new prepared pyrazole azo dye derivative (PY).

Here, we studied the inhibition properties of new prepared pyrazole azo dye derivative (PY) for carbon steel corrosion in 1.0 M HCl solution. In this study we used both experimental (i.e. electrochemical measurements) and theoretical studies to verify the investigations.

2 Experimental

2.1 Electrode and electrolyte

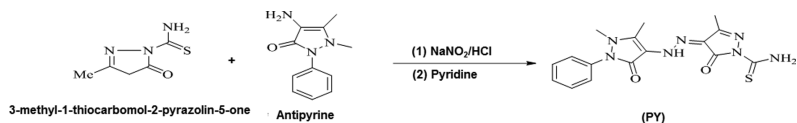
The C-steel specimens (Origin: Egyptian steel company) with formula (wt %): C (0.18), Si (0.08), Mn 0.35), P (0.17) and Fe (Rest) act as a working electrode. Its dimension is 2.0 cm × 1.0 cm × 0.05 cm. The surface of electrodes were prepared a corroding to ASTM G1 – 03(2017)e1.

The acidic electrolyte is 1.0 M HCl solution (Sigma-Aldrich).

2.2 Inhibitor (PY) synthesis

In glass flask, 2.03 g Antipyrine mixed with 3.0 mL HCl (37%), 2.0 mL distilled water at 278 K. This mixture was diazotized with NaNO₂ solution (0.7 g in 10 mL H₂O). The produced mixture was added drop wise 3-methyl-1-thiocarbomol-2-pyrazolin-5-one (0.01 M) in the presence of 15 mL pyridine (see Scheme 1). The complete reaction was obtained after 2 h stirring at 278 K. The final compound was obtained after filtration and washing with distilled H₂O and recrystallization from ethanol. The yield of this process is 74% and melting point of the prepared compound is 504 K. The purity of PY is confirmed by thin-layer chromatography (TLC).

The inhibitor synthesized was recognized by ¹H-NMR using a Bruker spectrometer at 300 MHz. The function groups for new compound was detected using Thermo Scientific FT-IR spectrometer.



Scheme 1: The synthetic procedure of pyrazole azo dye derivative (PY).

2.3 Electrochemical measurements

The performance of new corrosion inhibitor was determined using the electrochemical techniques (i.e. potentiodynamic polarization and EIS). Standard practice for electrochemical measurements including the cell and the methods were conducted according to ASTM G3 – 14. The potentials of polarization experiments were measured versus saturated (Hg/Hg₂Cl₂) (SCE). Three repeat experiments were carried out for all measurements.

The Electrochemical researches were achieved via Potentiostat/Galvanostat instrument (Gamry PCI4G750).

2.4 Quantum parameters

Quantum parameters were calculated to find the linkage between the inhibition character of PY compound and its structure. In this regards we used VAMP module (Materials Studio–Accelrys).

3 Result and discussion

3.1 The structure identity of PY

The IR spectrum (Figure 1) of PY exhibited absorption bands at 3337, 3265 and 3214 cm⁻¹. These bands refer to the NH₂ and NH groups [17]. The two absorption bands at 1653 and 1636 cm⁻¹ refer to the two carbonyl groups. The band at 1602 cm⁻¹ refer to the C=N group.

The ¹H NMR spectrum (Figure 2) displayed signals at 2.19, 2.51 and 3.14 ppm due to methyl protons of two pyrazole rings. The multiplet signals at 7.39–7.58 ppm refer to the aromatic protons. The two signals at 8.00 and 10.35 ppm refer to the NH₂ and tautomeric OH groups, respectively.

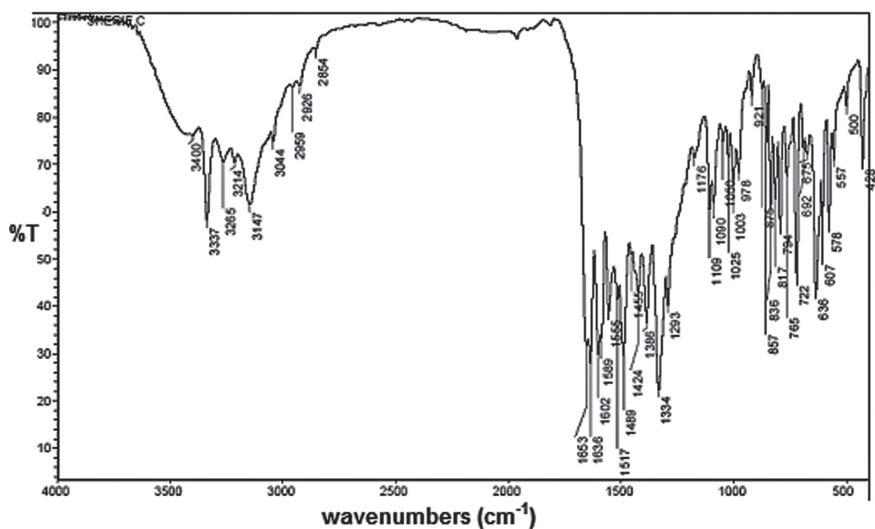


Fig. 1: FTIR spectra of prepared PY compound.

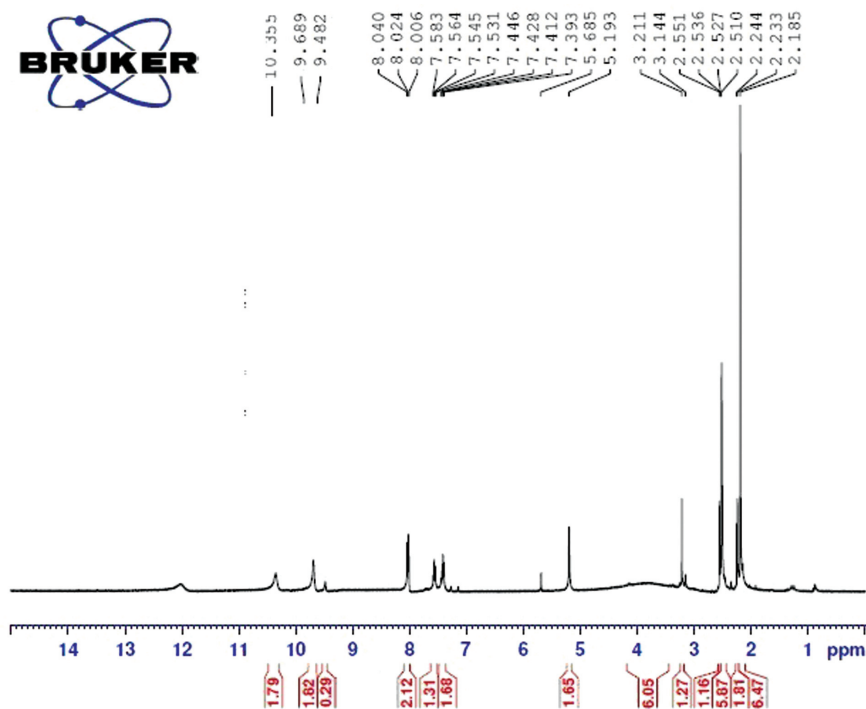


Fig. 2: The ¹H NMR spectrum of prepared PY compound.

3.2 Electrochemical studies

The inhibition performance of PY for C-steel corrosion in acid electrolyte (1.0 M HCl) was inspected using polarization method. Figure 3 shows the Tafel curves (the potential range ± 250 mV vs. OCP and scan rate = 0.5 mV s^{-1}) for blank and PY at 298 K.

Table 1 represents the polarization parameters, rest potential (E_{corr}) and corrosion current (I_{corr}) and Tafel slopes (β_a , β_c). The inhibition efficiency ($E_p\%$) of PY is calculated using equation 1 [18–20].

$$E_p\% = \frac{I_{\text{corr}(0)} - I_{\text{corr}}}{I_{\text{corr}(0)}} \times 100 \quad (1)$$

here $I_{\text{corr}(0)}$ represents the corrosion current for blank solution.

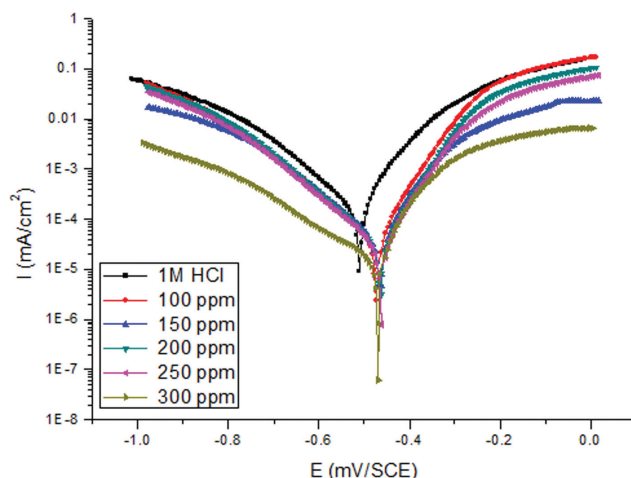


Fig. 3: Potentiodynamic polarization curves for carbon steel in 1.0 M HCl in absence and presence of various concentrations of PY at 298 K.

Tab. 1: Polarization parameters and the corresponding corrosion inhibition efficiency for carbon steel in 1.0 M HCl in the absence and presence of PY at 298 K.

C_{inh} (ppm)	I_{corr} ($\mu\text{A cm}^{-2}$)	$-E_{\text{corr}}$ (mV vs. SCE)	β_a (mV/dec.)	β_c (mV/dec.)	E_p (%)
0	160.5 ± 5	510.92 ± 8	82.20	137.80	0.00
100	43.6 ± 3	473.01 ± 6	74.60	139.50	72.81
150	36.82 ± 3	464.28 ± 5	72.70	136.70	77.06
200	31.25 ± 3	463.45 ± 5	71.80	130.30	80.53
250	26.96 ± 1	463.01 ± 3	73.10	133.60	83.20
300	13.66 ± 1	470.79 ± 4	59.80	182.70	91.50

We concluded from above data that the corrosion rate of C-steel in 1.0 M HCl decreased significantly with the addition of a variable dose of PY. The greatest efficiency (91.5%) (See Table 1) has been obtained at 300 ppm of PY. The movements of E_{CORR} in the case of inhibited solutions are less than 85 mV, indicating that the PY is mixed type inhibitor with more control of anodic reaction [21–23].

The changes in the values of Tafel slopes (β_a , β_c) after adding PY are insignificant. This confirms that the main mechanism of corrosion inhibition by PY is the blocking the active sites over the metal surface [24–26].

EIS responses were conducted to support the potentiodynamic polarization. The EIS spectra (i.e. Nyquist and Bode) for this system are shown in Figure 4.

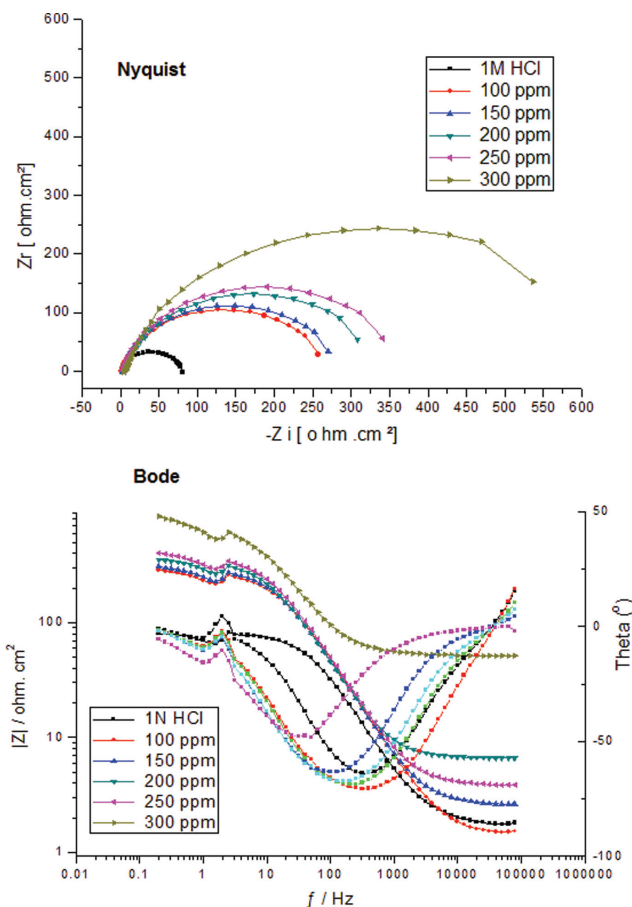


Fig. 4: EIS spectra for carbon steel in 1.0 M HCl in absence and presence of various concentrations of PY at 298 K.

In this case the EIS experiments were conducted at OCP in the frequency zone 0.1 Hz-100 kHz. The experiments start after 1 h of electrode insertion. The supposed equivalent circuit for this system is shown in Figure 5. It contains charge transfer resistance (R_{ct}), electrolyte resistance (R_{sol}) and dielectric capacitance (Q). These parameters are registered in Table 2.

The inhibition effectiveness ($E_R\%$) of PY is estimated using equation 2 [27–29].

$$E_R\% = \frac{R_{ct} - R_{cto}}{R_{ct}} \times 100 \quad (2)$$

here R_{cto} represents the charge transfer resistance for blank solution.

The addition of PY to 1.0 M HCl produces the accretion in R_{ct} values and the reduction in Q values (see Figure 4). This confirms the inhibitory effective of PY. Where, H_2O molecules over the C-steel surface were exchanged by PY molecules, causing the extension in the thickness of the electrical double layer [30–33]. The “n” values fall in 0.9 and 0.8 range (Table 2) indicates that this case is not the ideal capacitor [34–36]. It was noted also that there are no significant changes in the “n” with and without PY molecules. It was noted that the $E_R\%$ increased with PY concentration (see Table 2). The efficiency of PY reached the maximum value

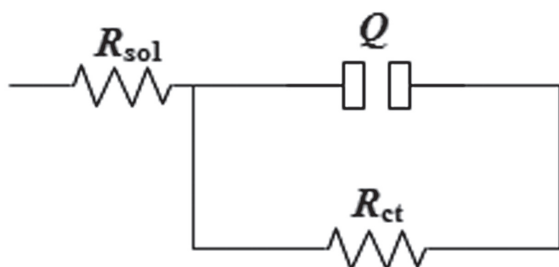


Fig. 5: The equivalent circuit the used to represent impedance data.

Tab. 2: EIS parameters and the corresponding corrosion inhibition efficiency for carbon steel in 1.0 M HCl in the absence and presence of PY at 298 K.

C_{inh} (ppm)	R_{sol} (Ω cm ²)	R_{ct} (Ω cm ²)	Q (μ F cm ⁻²)	n	E_R (%)
0	1.81 ± 0.4	74.75 ± 3	81.40	0.90	0.00
100	1.49 ± 0.4	252.0 ± 3	65.24	0.88	70.30
150	2.65 ± 0.2	268.9 ± 6	68.82	0.88	72.20
200	6.60 ± 0.2	312.1 ± 7	75.03	0.88	76.00
250	3.87 ± 0.3	347.2 ± 3	68.45	0.88	80.00
300	5.23 ± 0.5	657.8 ± 4	77.71	0.82	88.60

at 300 ppm. The inhibition efficiency of PY from EIS method complies with that from polarization method.

3.3 Quantum studies

The optimized structure of PY molecule was given in Figure 6. Both HOMO and LUMO regions (see Figure 7) are focused on sulfur, oxygen and nitrogen atoms

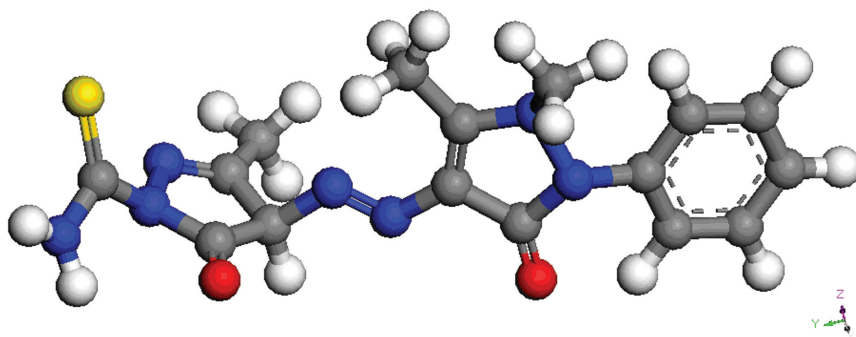


Fig. 6: The optimized structure of PY molecule.

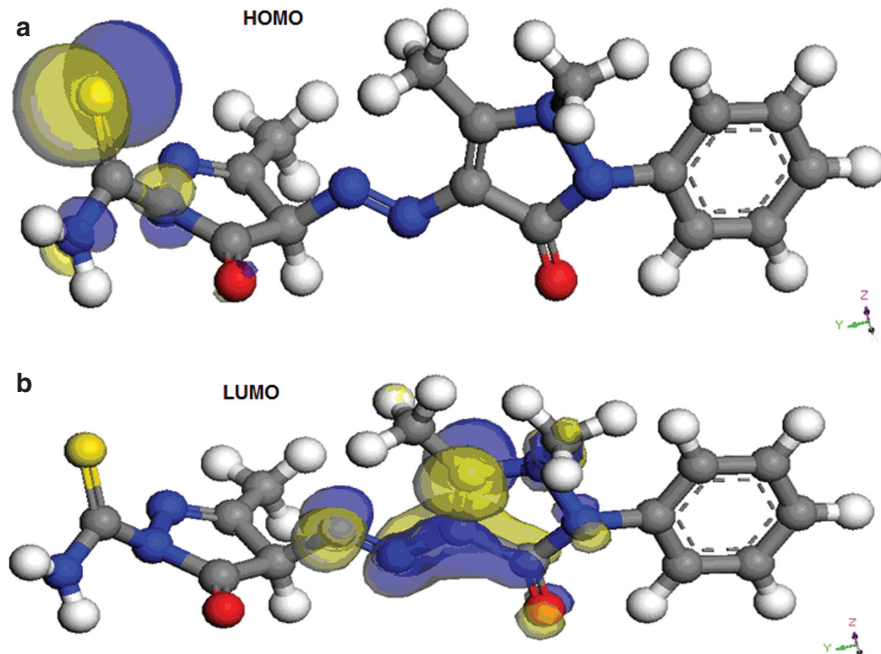


Fig. 7: HOMO (a) and LUMO (b) distributions in PY molecule.

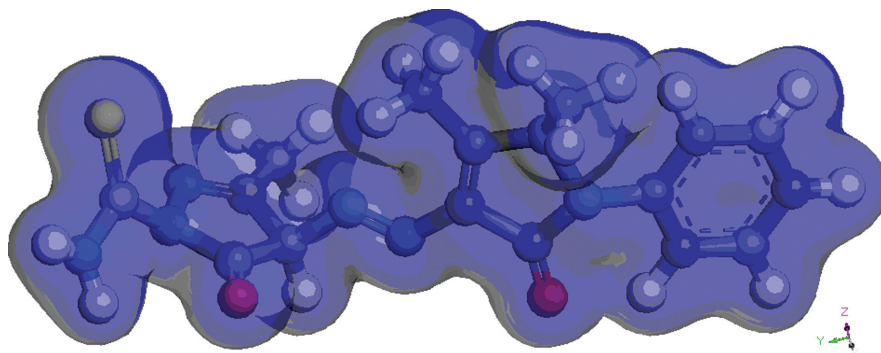


Fig. 8: The electron density is distributed over the whole PY molecule.

where HOMO is localized on sulfur atom while LUMO is distributed over the oxygen and nitrogen atoms. This indicates that the S, O and N atoms are the functional parts in PY molecule. The high value of E_{HOMO} (-8.912 V) means the susceptibility of the PY to supply electrons to unoccupied d-orbitals of Fe atom, forming a coordinate bond [37–39]. The low value of E_{LUMO} (-1.324 eV) means the susceptibility of the PY molecule to accept electrons from filled Fe d-orbital [40]. The low value of energy gap ($\Delta E = 7.588$ eV) suggests the high inhibition efficiency. The electron density moves over the whole PY (Figure 8), suggests that adsorption of PY on the steel surface occurs by flat-lying orientations [41–44].

3.4 Mechanism of action of pyrazole derivative

From the above results, we concluded that the main step in mechanism action of PY to control the degradation of C-steel in 1.0 M HCl is the adsorption process. The performance of pyrazole derivative depends mainly on the chemical structure of the PY. The surface charge plays a great role beside the potential of zero charge (pzc) of steel in acid solution in the inhibitor efficacy [45–50]. Generally, the surface of carbon steel is almost positively charged in acidic solutions [51].

In this status, PY molecules could be adsorbed on the C-steel surface by the interaction between π electrons in benzene ring or lone pair electrons of O, N and S atoms and the unfilled d -orbital of Fe surface atoms [52–55]. Based on this assumption, pyrazole derivative PY control C-steel dissolution by adsorbing on the corroding sites of metal and isolate its exposure to the acid solution (1.0 M HCl).

4 Conclusions

4-(2-(1,5-dimethyl-3-oxo-2-phenyl-2,3-dihydro-1H-pyrazol-4-yl)hydrazono)-3-methyl-5-oxo-4,5-dihydro-1H-pyrazole-carbothioamide (PY) was prepared, and its chemical structure was proven using spectroscopic techniques. The corrosion of C-steel in 1.0 M HCl has been inhibited via pyrazole derivative PY. The inhibition performance was reached to 91.50% at 300 ppm concentration. According to E_{corr} , PY molecules affected both anodic and cathodic reactions. Quantum calculations were utilized to support the experimental data and the adsorption behavior of pyrazole derivative PY.

References

1. Q. Zhang, Z. Gao, F. Xu, X. Zou, *Colloids Surf. A.* **380** (2011) 191.
2. M. A. Deyab, R. Essehli, B. El Bali, *RSC Adv.* **5** (2015) 48868.
3. M. A. Deyab, K. Eddahaoui, R. Essehli, S. Benmokhtar, T. Rhadfi, A. De Riccardis, G. Mele, *J. Mol. Liq.* **216** (2016) 699.
4. M. A. Deyab, S. T. Keera, *Egypt. J. Pet.* **21** (2012) 31.
5. I. B. Obot, N. O. Obi-Egbedi, N. W. Odozi, *Corros. Sci.* **52** (2010) 923.
6. S. Muralidharan, M. A. Quraishi, S. V. K. Iyer, *Corros. Sci.* **37** (1995) 1739.
7. F. Bentiss, M. Lebrini, M. Lagrenee, M. Traisnel, A. Elfarouk, H. Vezin, *Electrochim. Acta* **52** (2007) 6865.
8. S. K. Shukla, M. A. Quraishi, *Corros. Sci.* **51** (2009) 1990.
9. A. K. Singh, M. A. Quraishi, *Corros. Sci.* **51** (2009) 2752.
10. M. A. Deyab, H. A. Abo Dief, E. A. Eissa, A. R. Taman, *Electrochim. Acta* **52** (2007) 8105.
11. M. A. Deyab, S. T. Keera, S. M. El Sabagh, *Corros. Sci.* **53** (2011) 2592.
12. A. M. Al-Sabagh, H. M. Abd-El-Bary, R. A. El-Ghazawy, M. R. Mishrif, B. M. Hussein, *Egypt. J. Pet.* **20** (2011) 33.
13. S. A. El-Assaly, *Der Pharma Chem.* **3** (2011) 81.
14. D. K. Yadav, M. A. Quraishi, *Ind. Eng. Chem. Res.* **51** (2012) 8194.
15. K. Tebbji, I. Bouabdellah, A. Aouniti, B. Hammouti, H. Oudda, M. Benkaddour, A. Ramdani, *Mater. Lett.* **61** (2007) 799.
16. P. Doharea, K. R. Ansaria, M. A. Quraishia, I. B. Obot, *J. Ind. Eng. Chem.* **52** (2017) 197.
17. R. Harode, T. C. Sharma, *J. Indian Chem. Soc.* **66** (1989) 282.
18. M. A. Deyab, *J. Taiwan Inst. Chem. Eng.* **58** (2016) 536.
19. G. Mu, T. Zhao, M. Liu, T. Gu, *Corrosion* **52** (1996) 853.
20. M. A. M. Deyab, *J. Surfactants Deterg.* **18** (2015) 405.
21. E. S. Ferreira, C. Giancomelli, F. C. Giacomelli, A. Spinelli, *Mater. Chem. Phys.* **83** (2004) 129.
22. G. Lyberatos, L. Kobotiatis, *Corrosion* **47** (1991) 820.
23. M. A. Deyab, K. Eddahaoui, R. Essehli, T. Rhadfi, S. Benmokhtar, G. Mele, *Desalination* **383** (2016) 38.
24. V. V. Torres, R. S. Amado, C. F. de Sá, T. L. Fernandez, C. A. da Silva Riehl, A. G. Torres, E. D'Elia, *Corros. Sci.* **53** (2011) 2385.

25. R. S. Goncalves, D. S. Azambuja, A. M. Serpa Lucho, *Corros. Sci.* **44** (2002) 467.
26. M. A. Deyab, B. El Bali, R. Essehli, R. Ouarsal, M. Lachkar, H. Fuess, *J. Mol. Liq.* **216** (2016) 636.
27. A. Saxena, D. Prasad, R. Haldhar, G. Singh, A. Kumar, *J. Mol. Liq.* **258** (2018) 89.
28. B. G. Prakashaiah, D. Vinaya Kumara, A. Anup Pandith, A. Nityananda Shetty, B. E. Amitha Rani, *Corros. Sci.* **136** (2018) 326.
29. M. A. Deyab, S. S. Abd El-Rehim, *Corros. Sci.* **65** (2012) 309.
30. E. A. Noor, *Mater. Chem. Phys.* **114** (2009) 533.
31. Q. B. Zhang, Y. X. Hua, *Electrochim. Acta* **54** (2009) 1881.
32. M. Behpour, S. M. Ghoreishi, N. Mohammadi, N. Soltani, M. Salavati-Niasari, *Corros. Sci.* **52** (2010) 4046.
33. M. A. Deyab, *Desalination* **384** (2016) 60.
34. M. Ozcan, F. Karadag, I. Dehri, *Colloids Surf. A* **316** (2008) 55.
35. E. E. Oquzie, Y. Li, F. H. Wang, *J. Colloid Interface Sci.* **310** (2007) 90.
36. A. Popova, E. Sokolova, S. Raicheva, M. Christov, *Corros. Sci.* **45** (2003) 33.
37. V. S. Sastri, J. R. Perumareddi, *Corrosion* **53** (1997) 617.
38. S. Martinez, *Mater. Chem. Phys.* **77** (2003) 97.
39. G. Gao, C. Liang, *Electrochim. Acta* **52** (2007) 4554.
40. W. Huang, Y. Tan, B. Chen, J. Dong, X. Wang, *Tribol. Int.* **36** (2003) 163.
41. T. Arslan, F. Kandemirli, E. E. Ebenso, I. Love, H. Alemu, *Corros. Sci.* **51** (2009) 35.
42. D. K. Yadav, B. Maiti, M. A. Quraishi, *Corros. Sci.* **52** (2010) 3586.
43. M. L. Zheludkevich, K. A. Yasakau, S. K. Poznyak, M. G. S. Ferreira, *Corros. Sci.* **47** (2005) 3368.
44. M. A. Deyab, *RSC Adv.* **8** (2018) 20996.
45. P. Mohan, G. Paruthimal Kalaighnan, *J. Mater. Sci. Technol.* **29** (2013) 1096.
46. N. D. Nam, Q. V. Bui, M. Mathesh, M. Y. J. Tan, M. Forsyth, *Corros. Sci.* **76** (2013) 257.
47. G. Moretti, F. Guidi, F. Fabris, *Corros. Sci.* **76** (2013) 206.
48. J. O' M. Bockris, A. K. N. Reddy, M. Gamboa-Aldeco (Eds.). *Modern Electrochemistry, Second Ed.*, Kluwer Academic, New York (2000), p. 919–920. p. 937, 968–972.
49. M. A. Deyab, *J. Solid State Electrochem.* **13** (2009) 1737.
50. M. A. Deyab, *Electrochim. Acta* **202** (2016) 262.
51. M. K. Pavithra, T. V. Venkatesha, K. Vathsala, K. O. Nayana, *Corros. Sci.* **52** (2010) 3811.
52. S. S. Abd El-Rehim, M. A. M. Deyab, H. H. Hassan, A. A. A. Ibrahim, *Z. Phys. Chem.* **230** (2016) 1641.
53. H. M. Abd El-Lateef, M. Ismael, A. H. Tantawy, *Z. Phys. Chem.* **230** (2016) 1111.
54. M. A. Abbas, M. A. Bedair, *Z. Phys. Chem.* **233** (2019) 225.
55. N. Dkhireche, A. Dahami, A. Rochdi, J. Hmimou, R. Tourir, M. Ebn Touhami, M. El Bakri, A. El Hallaoui, A. Anouar, H. Takenouti, *J. Ind. Eng. Chem.* **19** (2013) 1996.